

ANALYSIS OF FOAM FILLED ROTOR SECTIONS

Luca S. Cecchini, Paul M. Weaver and Christopher J. Biggs
Department of Aerospace Engineering, Queens Building, University of Bristol
Bristol, UK, BS8 1TR
luca.cecchini@bristol.ac.uk

Abstract

Modern, thin shell structures, such as rotor blades, are efficient at carrying bending loads due to the significant proportion of material far from neutral axes. However by keeping such structures hollow, they have been left vulnerable to through section crushing forces. This paper looks at the effect of the Brazier effect on such shell structures and the potential for core fillings to prevent structural collapse. Analytical models are produced, for filled orthotropic circular cylindrical tubes, with which the benefits of core fillings can readily be determined.

It is found that Rohacell foam, commonly used in mandrels for manufacturing, is extremely effective at preventing tube collapse, and that it has the potential to provide weight savings in structures where bending is a principle load case.

Introduction

Since Brazier (Ref 1) it has been recognised that long, slender, shell structures, such as rotor blades, exhibit non-linear behaviour due to through section forces, when bending loads are applied. Inward acting loads, a consequence of the curvature of the beam (von-Karman, Ref 2), cause a reduction in the cross-sectional second moment of area, and thus a reduction in bending stiffness of the structure. The curvature, for a given applied load, will therefore be greater than simple linear beam theory predicts.

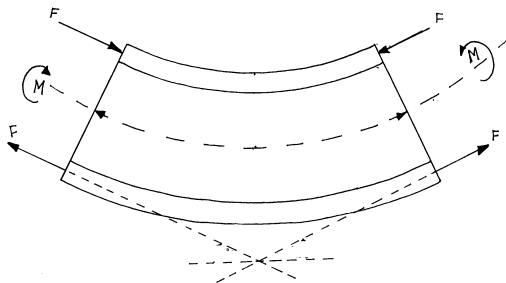


Fig. 1 Through section loads due to curvature

of circular cylinders), and will eventually lead to a collapse of the structure as the reduced second moment of area is no longer able to withstand the applied load. An alternative, parallel, explanation is the desire of the structure to reduce its internal energy by moving material towards its neutral axis, thus reducing surface stresses.

The relatively simple initial analysis on hollow tubes, by Brazier, was later extended to include higher order terms by Reissner (Ref 3 & 4) and Reissner and Weingarten (Ref 5). Kedward (Ref 6) and Stockwell and Cooper (Ref 7) have extended Brazier and Reissner's analyses (respectively), to include orthotropic effects. This has subsequently been followed by Tatting *et al.* (Ref 8 & 9); whose analyses are based on Vlasov's semi-membrane theory, and Harursampath and Hodges (Ref 10) who carried out an extremely thorough, asymptotically correct, analysis of the problem. Particular note is made of Calladine's (Ref 11) excellent analysis of the problem, which reformulated Brazier's solution into a more manageable form, reducing the problem to one variable.

Solid beams do not exhibit such phenomena as the material within the section prevents its flattening. Similarly, multi-bay rotor blade structures, with their vertical supports (such as spars) have mechanisms to resist such flattening. However, large bays or thin walled sections, such as trailing edges, remain susceptible to the Brazier effect.

Core fillings, such as Rohacell foam or Aluminium / Nomex honeycombs, are widespread in the rotor industry, both as mandrels for manufacturing, and to provide support for aerodynamic loads. Karam and Gibson (Ref 12) have looked at the effect of cores on shell structures, with particular focus on organic structures, such as plant stems. Their analysis looked both at their affect on local buckling, as well as the Brazier effect. It is the hope of this paper to combine a modified version of Karam and Gibson's analysis to Kedward's simple analysis of orthotropic tubes to determine the potential performance improvements provided by core fillings within hollow structures. Karam and Gibson's analysis, itself, is based on the work of Calladine.

The cross-sectional deformation manifests itself as a flattening of the cross-section (ovalisation in the case

Notation

Throughout, the following notation will be used, based on that used by Calladine;

- | | | |
|---------------|---|----------------------------------|
| a | : | radius of the tube |
| c | : | curvature of the tube |
| t | : | shell thickness |
| v | : | circumferential displacements |
| w | : | radial displacements |
| | | |
| E | : | Young's modulus |
| G | : | shear modulus |
| I | : | second moment of area |
| S | : | shear modulus |
| | | |
| $[a]$ | : | Compliance matrix |
| | | |
| $[A]$ | : | shell in-plane stiffness matrix |
| $[D]$ | : | shell bending stiffness matrix |
| | | |
| ε | : | strain |
| θ | : | angle to neutral axis of bending |
| ζ | : | section flattening |

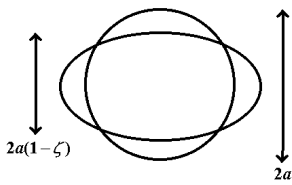


Fig. 2a Section flattening

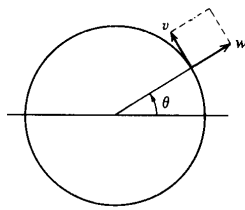


Fig. 2b Displacements

Analysis

Rotor blades are complex structures, although long and generally prismatic in the longitudinal direction, varying curvatures and wall thicknesses (in the cross-section), bayed designs and sharp trailing edges all add complications to their analyses. In this study, the problem is therefore simplified to that of a circular cylindrical shell, in keeping with the general trend in the literature. Other hollow structures have been analysed under such bending, including rectangular (Timoshenko, Ref 13), elliptical (Huber, Ref 14) and multibay (Paulson and Welo, Ref 15) cross-sections.

In line with Vlasov's (Ref 16) semi-membrane theory, the shell is assumed to remain inextensional in the circumferential direction, and longitudinal bending of the shell wall (D_{11}) is assumed to have little effect on the deformation of the structure. FE studies by Stockwell and Cooper and the current authors

confirm the circumferential inextensionality hypothesis. Therefore

$$w + \frac{\partial v}{\partial \theta} = 0$$

The ovalisation of the structure suggests a doubly periodic deformation, and thus a first order approximation of shell deformation can be given by,

$$w = a\zeta \cos 2\theta$$

(1)

and hence

$$v = -\frac{1}{2} a\zeta \sin 2\theta$$

(2)

Fig. 3 is the resulting deformed shape for a long aluminium tube in FE (ABAQUS / STANDARD) and using the above equations, for a deformation with the same ζ .

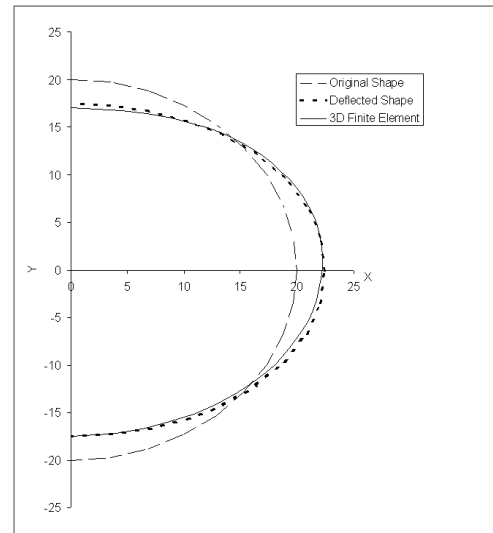


Fig. 3 Deformed structure comparison of FE and analytical model.

As can be seen, the deformed shape is predicted quite accurately. The non-symmetry can be attributed to a combination of Poisson's effects from longitudinal bending, and shell wall bending (D_{11}). The assumed deformation shape is therefore used.

If the form of the shell displacement is assumed to be unaffected by the foam core, then by assuming a constant strain through the core it is possible to calculate the energy of deformation of the core.

Through section radial strains of the core are given by

$$\varepsilon_{r(c)} = \zeta \cos 2\theta \quad (3)$$

$$\varepsilon_{\theta(c)} = 0 \quad (4)$$

$$\gamma_{r(c)} = -2\zeta \sin 2\theta \quad (5)$$

The presence of core material all the way, lengthwise, down the tube, prevents net longitudinal strains, however the foam is partially free to expand in the circumferential direction (due to Poisson's coupling of radial strains). Since the core will expand circumferentially in areas of radial compression, and contract in areas of tension, the structure will "bow" rather than remain rigid, only failing to strain close to the shell.

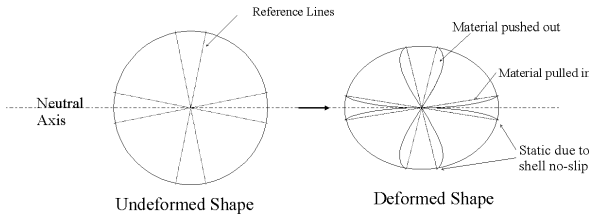


Fig. 3 Material bowing due to Poisson's effects

This extra degree of freedom reduces the internal energy of the foam, and results in only one direction of plane strain. The energy of deformation of the core through the section is therefore given by

$$U_c = \frac{\pi}{4} \left(\frac{E_c}{1-\nu_c^2} + 4G_c \right) (a - \frac{1}{2})^2 \zeta^2 \quad (6)$$

where the Young and shear moduli are kept separate, as the isotropic $E=2G(1+\nu)$ relationship is not necessarily valid for foams or other "structural" cores.

Using, from Calladine,

$$\kappa_\theta = -\frac{1}{a^2} \left(w + \frac{\partial^2 w}{\partial \theta^2} \right),$$

the energy of circumferential bending (ovalisation) of the shell can be calculated to be

$$U_{circ(shell)} = \frac{9D_{22}\pi\zeta^2}{2a} \quad (7)$$

The reduction in second moment of area of the shell (and core) can be calculated (from Eqn 1 & 2) to be

$$I = I_0 \left(1 - \frac{3}{2}\zeta + \frac{3}{8}\zeta^2 \right) \quad (8)$$

However, in line with Brazier's removal of higher order terms, the ζ^2 term are removed. Calladine has shown that the combination of this and the simplified displacement assumption (Eqn 1), actually combine to produce a surprisingly accurate result.

Thus the energy of longitudinal bending of the tube (including the foam core) is given by

$$U_{long} = \frac{1}{2} c^2 \pi \left(1 - \frac{3}{2}\zeta \right) \left[\left(A_{11} - \frac{A_{12}^2}{A_{22}} \right) a^3 + E_c (a - \frac{1}{2})^4 \right] \quad (9)$$

There is a further energy associated with the interaction of different Poisson's ratios in the shell and core, however if they are of a similar value then this can be assumed negligible. By differentiating the total energy with respect to ζ , and equating to zero, it is possible to find the lowest energy deformation, and hence the preferred deformation state.

$$\zeta = \frac{c^2 a \left[\left(A_{11} - \frac{A_{12}^2}{A_{22}} \right) a^3 + E_f (a - \frac{1}{2})^4 \right]}{12D_{22} + \frac{4}{9} \left(\frac{E_f}{1-\nu^2} + 4G_f \right) (a - \frac{1}{2})^2 a} \quad (10)$$

Combined with Eqn 9 this can be used to find the bending moment curvature relationship

$$M = c\pi \left[\left(A_{11} - \frac{A_{12}^2}{A_{22}} \right) a^3 + E_c (a - \frac{1}{2})^4 \right] \times \left[1 - \frac{c^2 a \left[\left(A_{11} - \frac{A_{12}^2}{A_{22}} \right) a^3 + E_c (a - \frac{1}{2})^4 \right]}{8D_{22} + \frac{4}{9} \left(\frac{E_c}{1-\nu_c^2} + 4G_c \right) (a - \frac{1}{2})^2 a} \right] \quad (11)$$

By substituting in Eqn 10 for the curvature terms, and differentiating with respect to ζ , the bending moment is found to peak at a $\zeta = \frac{2}{9}$. This is the maximum load the structure can take, assuming that neither, material nor local buckling, failures occur first. This value is irrespective of lay-up or the composition of the core.

If the shell is assumed to be thin ($a \gg t$) and a_{11} is defined as (in orthotropic materials)

$$\frac{1}{a_{11}} = A_{11} - \frac{A_{12}^2}{A_{22}}$$

then the resulting equation is simplified to

$$M = c\pi a^3 \left[\frac{1}{a_{11}} + E_c a \right] \left(1 - \frac{c^2 a^4 \left[\frac{1}{a_{11}} + E_c a \right]}{8D_{22} + \frac{4}{9} \left(\frac{E_c}{1-\nu_c^2} + 4G_c \right) a^3} \right)$$

The large cross-sectional deformations produce large strains in the core. In the case of foam cores, these may fail at strains of between 1% (for a brittle aerospace foams) to almost 100% (compression) strain (for a household sponge). If this failure strain is reached before $\zeta = \frac{2}{9}$, then the core will gradually begin to fail, starting with the areas at 0° and 90° to the neutral axis in direct strain, and 45° in shear. Thus if the structure is limited to $\zeta < \varepsilon_{\max(\text{core})}$ the core will not be damaged, but this will severely limit the performance of the structure. The actual deformation at structural collapse will lie between

$$\frac{2}{9} \geq \zeta_{\max} \geq \begin{cases} \varepsilon_{\max} \\ \frac{1}{2} \gamma_{\max} \end{cases}$$

However, work by various author (Brazier and Corona & Rodrigues, Ref 17) suggests that a hollow structure will fail either by material or local buckling before the Brazier limit moment is reached. Thus the maximum allowable deformation is likely to be less than $\zeta = \frac{2}{9}$. However, the presence of foam acts as an elastic foundation, preventing local buckling, as well as a stiffening against ovalisation. This later factor will further increase local buckling loads, as the critical stresses are dependent upon local shell curvature (Calladine).

Performance effects

Having obtained simple mathematical models to represent the behaviour of filled tubes, the effect of their presence is investigated. Aircraft design optimisation is often directed towards the minimisation of the mass of structures, in order to maximise payload or performance capabilities. Rotor blades are rather more complex, as they must fulfil various dynamic criteria, and must have a certain mass. None-the-less, reduction of structural mass to resist bending loads can allow the application of

increased stiffening in other directions, or improved mass distribution to improve dynamic characteristics. The principle objective of the subsequent work is to look at the mass / failure load ratios as a benchmark for performance.

The study will not investigate material or local buckling type failures, however the prevention of Brazier type non-linearities will lead to increases in loads to failure, particularly circumferential material failure due to cross-sectional deformation of the shell.

Reference Tube

The analysis is based around a 20mm radius, 1mm wall thickness CFRP tube, with various grades of Rohacell foam as cores. Both the materials and the dimensions are typical of those used in rotor blade manufacture. The behavioural properties of both are listed in Appendix 1. Since this study focuses on orthotropic shells, the layup is $[90^\circ-0^\circ]_s$.

The tube geometry was selected to be typical of thin walled rotor section (20:1 radius to wall ratio).

Retention of linear behaviour

By preventing ovalisation, the presence of a core structure will extend the linear behaviour region of the tube and, assuming an infinite core strain limit, will increase the ultimate Brazier collapse moment of the structure.

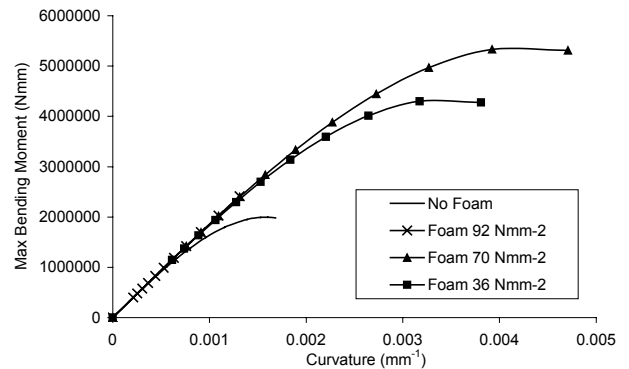


Fig 4 Bending curvature for infinite elastic limit cores

The increase in performance is significant, however, as previously mentioned, most cores will exhibit some form of material failure before $\zeta = \frac{2}{9}$ is reached. Thus by finding the limit moment at $\zeta = \varepsilon_{\max(\text{core})}$, (from material property sheets) the behaviour up to the initiation of damage can be investigated. This represents a limit (not ultimate) load for the structure, and a certain reserve factor will still remain.

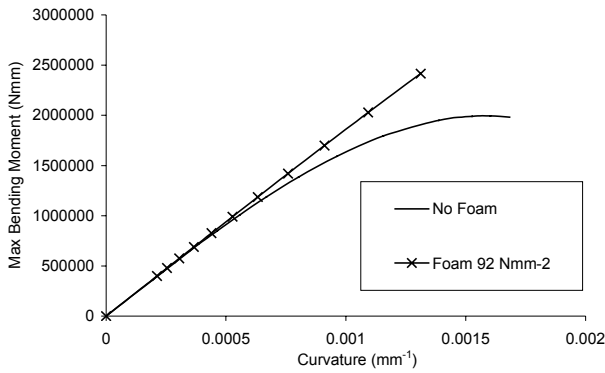


Fig 5 Bending curvature up to core failure

The end of the line represents the point of material failure initiation in the core. Up to the elastic limit of Rohacell foam the tube seems to bend in a linear manner. This is to be expected as, at failure in 92 Nmm⁻² Rohacell, ζ is only 0.016. Despite this substantial limitation on the structure, it still outperforms the reference hollow tube.

Optimisation of ply angle

In recent work by the current authors (Ref 18), it has been demonstrated that the maximisation of the Brazier moment, in composite tubes, is achieved by a three layer composite consisting of a 90°-0°-90° lay-up, with, in general, a 60% ratio of 0° to 90° plies. However, the presence of a foam core can provide significant reinforcement against core collapse, thus reducing the necessity for circumferential plies. The optimum ply ratio will therefore tend towards an all 0° layup. Fig. 6 shows this effect graphically in 90°-0°-90° laminates, assuming collapse at $\zeta = \frac{2}{9}$. As can be noted the presence of a Rohacell core changes the optimum configuration of the shell to consist purely on 0° plies, a pattern maintained even with ζ limited to the cores maximum strain.

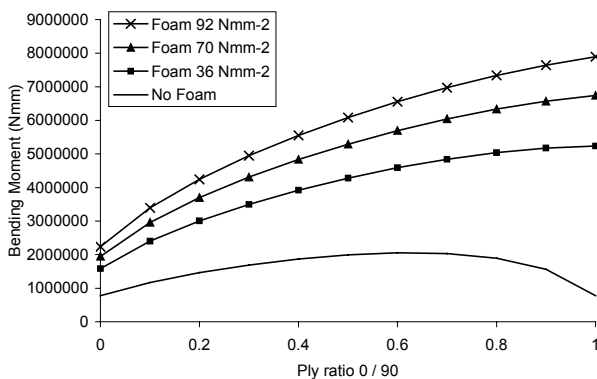


Fig. 6 Optimisation of performance with ply ratio

Minimisation of weight

As previously stated, the important benchmark to measure whether the presence of a foam core can improve performance, is that of mass optimisation. The presence of, albeit light, material filling the large volume inside a thin shell structure, can cause a significant increase in structure mass. To study this, the reference radius tube is designed to carry a certain load, using the optimum ply configurations, by varying the wall thickness until the required failure load is met. The mass of these tubes (per unit length) is then calculated. This is carried out, in the case of filled tubes, both with $\zeta_{\max} = \frac{2}{9}$ and $\zeta_{\max} = \epsilon_{\max(\text{core})}$.

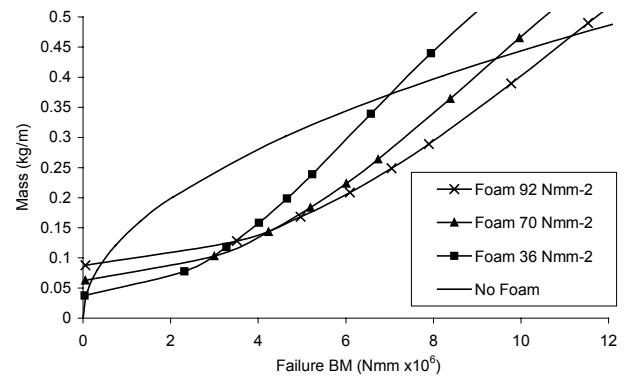


Fig 7a Mass per failure load $\zeta_{\max} = \frac{2}{9}$

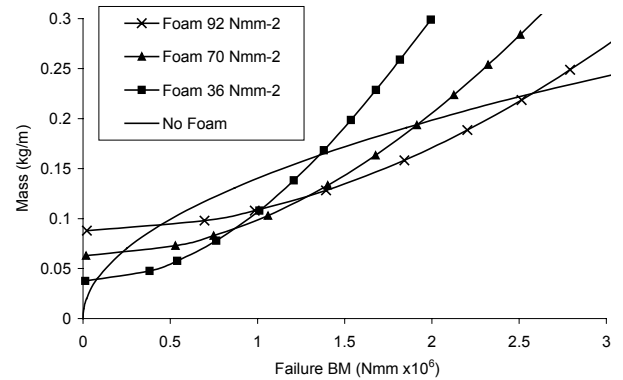


Fig7b Mass per failure load $\zeta_{\max} = \epsilon_{\max}$

In the plots, the filled tubes are initially less efficient, as the core structure is substantially heavier than the shell, and the tube behaves more like a solid. However, as the shell mass increases, (with increasing bending load), the cores begin to become more mass efficient. Eventually, however, the thickness to radius ratio again increases such that the cores circumferential stiffness is small compared to the shell's, once again rendering it inefficient.

The cross-over point for the 92 Nmm⁻² foam (where it again becomes less efficient than the hollow shell), occurs at a radius to thickness ratio of 20:1 in the hollow shell (around 1:30 in the filled shell).

Maintaining a constant radius, is analogous to designing to a given cross-sectional (possibly aerodynamically defined) shape, as would occur in rotor blade design. The actual optimal configuration is, predictably, dependent on the desired failure load. However, the cores can, certainly, provide a mass efficient method of reinforcement.

Conclusions

Modern day rotor blades are complex composite shells which often have foam (typically Rohacell) or Honeycomb (aluminium or Nomex) cores. Aside from their use as mandrels in manufacturing, these will provide significant through section reinforcement against both aerodynamic and Brazier type loads. The summarised work has provided simple models for the analysis of the non-linear bending of such structures. Due to the small curvatures experienced by rotor blades in flight, these effects are unlikely to manifest themselves in normal conditions. However in extreme cases, for example due to impacts, large displacements may occur. In such cases, an understanding of such non-linear bending, and the function of foam cores in their support, should be valuable.

Acknowledgements

The authors would like to thank EPSRC and Westland Helicopters for their support in this research.

Appendix 1: Material properties

Properties	Units	Rohacell		
		31	51	71
Density	kg/m ³	30	50	70
Tensile Strength	N/mm ²	1.0	1.9	2.8
Compression Strength	N/mm ²	0.4	0.9	1.5
Shear Strength	N/mm ²	0.4	0.8	1.3
Modulus of Elasticity	N/mm ²	36	70	92
Shear Modulus	N/mm ²	14	21	30
Poisson's ratio		0.3	0.3	0.3

Fig A.1 Rohacell foam properties

Properties	Units	CFRP
Density	kg/m ³	1600
E ₁₁	N/mm ²	140000
E ₂₂	N/mm ²	10000
G ₁₂	N/mm ²	5000
ν ₁₂		0.3

Fig A.2 CFRP properties

References

1. Brazier, L.G. (1927) On the flexure of thin cylindrical shells and other 'thin' sections. *Proceeding of the Royal Society of London, Series A*, **116**, 104-14.
2. von-Kármán, T. (1911) Ueber die formänderung dünnwandiger Rohre, insbesondere federnder Ausgleichrohre. *Zeit. Des Vereines deutscher Ingenieure*, **55**, Nr 45, 1889-1895.
3. Reissner, E. (1959) On finite bending of pressurised tubes, *Journal of applied Mechanics* **26**, 386-392.
4. Reissner, E. (1961) On finite bending of cylindrical tubes, *Ingenieur Archiv*, **15**, 165-172.

5. Reissner, E. and Weinitschke, H. J. (1963) Finite bending of circular cylindrical tubes, *Quarterly of Applied Mathematics* **20**, Nr. 4 305-319
6. Kedward, Keith T. (1978) Non-linear Collapse of thin-walled composite cylinders under flexural loading, *Proc of the Int Conf on Composite Materials*, 2nd, p 353-365.
7. Stockwell, A.E. and Cooper, P. A. (1992) Collapse of composite tubes under bending, *Proceedings of the 33rd Structures, Structural Dynamics and Materials Conference*, 1841-1850.
8. Tatting B.F., Gurdal Z. and Vasiliev V.V. (1996), Nonlinear response of Long Orthotropic Tubes Under Bending Including the Brazier Effect, *AIAA Journal*, **34**, Nr. 9 1934-1940
9. Tatting B.F., Gurdal Z. and Vasiliev V.V. (1997) The Brazier effect for finite length composite tubes under bending, *International Journal of Solids & Structures* **34**, 1419-1440
10. Hodges D.H. (1999) Asymptotic analysis of the non-linear behaviour of long anisotropic tubes, *International Journal of Non-linear Mechanics* **34**, 1003-1018.
11. Calladine C.R. (1983) Theory of shell structures, *Cambridge University Press, Cambridge*.
12. Karam, G. N. and Gibson, L. J. (1995), Elastic buckling of cylindrical shells with elastic cores; Part I: Analysis. *International Journal of Solids and Structures*, **32**, 1259-1283.
13. Timoshenko, S, (1923) Bending Stresses in Curved Tubes of Rectangular Cross-section. *Transactions of the American Society of Mechanical Engineers*, **45**, 135-140
14. Huber, M. T. (1948) The Bending of Curved Tube of Elliptic Sections. *Proceedings of the Seventh International Congress for Applied Mechanics*, 322-328.
15. Paulsen, F. and Welo, T. (2001), Cross-sectional Deformations of Rectangular Hollow Sections in Bending: Part II, analytical models. *International Journal of Mechanical Sciences*, **43**, 131-152.
16. Vlasov, V.Z. (1949), Obshchaya teoriya obolochek I yeye prilozheniya v tekhnike; *Translation* (1964), General theory of Shells and its applications to engineering, *NASA Technical Translation TT F-99*.
17. Corona, E. and Rodrigues, A. (1995) Bending of long cross-ply composite cylinders. *Composites Engineering*, **5**, Nr 2, 163-182.
18. Cecchini, L.S. and Weaver, P.M. (2002), Optimal fibre angles to resist the Brazier Effect in Orthotropic tubes. *Accepted for publication as technical note in AIAA Journal*, 2002.